

Synthetic Pulp Fiber Ozonation: An ESCA and FTIR Study

H. CHTOUROU,¹ B. RIEDL,^{1*} B. V. KOKTA,² A. ADNOT,³ and S. KALIAGUINE³

¹Centre de Recherche en Sciences et Ingénierie des Macromolécules (CERSIM), Département des sciences du bois, Faculté de Foresterie et de Géomatique, Université Laval, Ste-Foy, Québec, G1K 7P4 Canada; ²Centre de Recherche en Pâtes et Papiers (CRPP), Université du Québec à Trois-Rivières, C.P.500, Trois-Rivières, Québec, G9A 5H7 Canada; ³Groupe de Recherche sur les Applications de la Physico-chimie des Surfaces (GRAPS), Faculté des Sciences et de Génie, Université Laval, Ste-Foy, Québec, G1K 7P4 Canada

SYNOPSIS

Polyethylene (PE) pulp fiber was treated by ozone for surface modification. Surface analysis was performed by using X-ray photoelectron (ESCA) and IR (FTIR) spectroscopies. Carbon (C) and oxygen (O) were the main atoms detected by ESCA (C_{1s} , O_{1s} regions) on the treated fiber. Analysis of the C_{1s} peaks (C1, C2, and C3) showed that the oxidation level changed with the ozonation time. O_{1s} peak components (O0, O1, and O2) were very useful to complete the surface analysis. FTIR spectra showed the presence of carbonyl groups ($1740\text{--}1700\text{ cm}^{-1}$), even on nontreated fiber, which increased in intensity as treatment time increased. Ozone treatment went beyond the surface level to the bulk of the fiber. This was marked by a large increase of the intensity of the carbonyl band after 3 h of ozonation. Thermal analysis suggests structure and morphology changes of fiber when exceeding 2 h of ozonation. © 1993 John Wiley & Sons, Inc.

INTRODUCTION

Pulp is the raw material for the production of paper, paperboard, fiberboard, and similar manufactured products. Wood is the principal origin of the pulp fiber produced around the world. Pulp fiber can be produced also by synthetic ways. Polyolefin synthetic pulps (polyethylene and polypropylene) are the most common and are designed to be blended in all proportions with wood pulp and made into papers using conventional equipment. As polyolefin surfaces are hydrophobic and not chemically bondable to other materials,¹ poor interfiber adhesion is the main problem with such composites and is greatly dependent on the surface properties of the blended materials. Thus, understanding the nature of surfaces and interfaces is an issue of major concern for these applications. For paper applications, the modification of synthetic fiber is required for bondability and water wettability and also for better adhesion with wood fiber as in composite papers.

However, an efficient, economical, and practical method to modify the surface of polyolefin fiber is needed to ensure market expansion.

For better interfiber bonding and water wettability and dispersion, a wide variety of water-soluble polymers or even conventional surfactants may be added before fiber making. Forbess et al.² showed that poly(vinyl alcohol) (PVA) is preferred especially for polyethylene (PE) pulps. These treatments provide only superficial wettability rather than true compatibility with lignocellulosic fiber.³ To improve compatibility, a mixture of unmodified polyolefins and copolymers of α -olefins and acrylic acid or maleic anhydride has been subjected to a spurling process as an aqueous emulsion to introduce polar groups in the resulting pulp.⁴ Chemical grafting of polar monomers, e.g., acrylamide, acrylic acid, and maleic anhydride, also has been reported.⁵⁻⁷ The increase of surface energy following the introduction of polar groups onto a nonpolar material improves adhesion. It is also possible to increase the surface energy by generation of polar groups through different techniques on polymeric surfaces, such as the corona discharge on poly(ethylene terephthalate) (PET) and PE films⁸⁻¹⁰ and UV light on PET,⁸ nylon 6, and polypropylene (PP)¹¹ films.

* To whom correspondence should be addressed.

Dasgupta¹ reported that ozonation of dilute aqueous slurry of PP pulp generates carboxyl groups, and this yields better responses toward paper wet-strength resins. However, the ozonation degraded the chain length of polyolefins as shown by the intrinsic viscosity of the treated material.¹

X-ray photoelectron spectroscopy or electron spectroscopy for chemical analysis (ESCA) involves the measurement of binding energies of electrons ejected by ionization of atoms with a monoenergetic beam of soft X-rays. It has been already used for the surface characterization of wood,^{12,13} wood pulp fiber,¹⁴⁻¹⁶ textiles,^{17,18} cellulose,^{15,19} and polymers²¹⁻²⁷ such as films preirradiated with UV radiation,²⁴ PE film modified by halogenated gas,²⁵ and PET film grafted with poly (acryl amide).²⁶

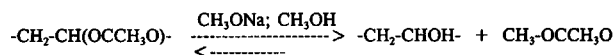
Infrared spectroscopy has been extensively used in the characterization of cellulose,^{27,28} lignin,^{29,30} and polymers.^{31,32} In recent years, with the advent of FTIR spectroscopy, surface sensitivity has improved but not as much as with ESCA. However, in systems with variable chemical composition within the surface depth range 0–1 μm , the two techniques are complementary.

The objective of this work was to study the effect of ozone treatment on PE pulp fiber, pretreated by a wetting water-soluble polymer, at the surface level and in the bulk, using ESCA and FTIR techniques.

EXPERIMENTAL

Materials

Synthetic pulp fiber used in this work was a PE fiber from DuPont. A wetting agent, apparently PVA, was previously introduced into the polymer solution before flash spinning. PVA is synthesized from poly(vinyl acetate) through an alcoholysis reaction:



This is seldom carried to completion. Hence, both hydroxyl and acetate groups should be present at the fiber surface.

Polyolefin pulp fiber has a very irregular surface with many crevices. It has a quite large specific surface area, typically 5–20 m^2/g , a high brightness (> 90%), and a bulk density of 0.2–0.4 g/cm^3 . PE pulp fiber was received as folded, thick, low-density sheets. It was washed with lukewarm water to dissolve any surface-adsorbed water-soluble polymer. The PE pulp fiber was then oven-dried and defi-

brated. An aspect ratio of 74 ± 59 ($L \approx 0.6$ mm, $d \approx 8$ μm) was measured.

Fiber Ozonation

The experimental procedure used for the ozonation of PE fiber was partially similar to the procedure described by Dasgupta.¹ The reaction was carried out in a cylindrical resin-making flask (1.5 L glass flask), with inlet and outlet tubes for gas flow and a stirrer (Fig. 1). The slurry containing around 3% fiber by weight (25 g of PE fiber/800 mL of water) was heated to $70 \pm 10^\circ\text{C}$ and well stirred while passing a regulated amount of ozone into the slurry. Two drops of surfactant (Tween 80) were added to the slurry to maintain a good dispersion of fibers in the water.

A Matheson laboratory ozonator, Model 8340, was used to generate ozone from oxygen at a power of 130 W and a pressure of 0.4 bar. An excess of potassium iodide solution was used to neutralize the amount of unreacted gas (ozone) leaving the reaction flask. Samples are described in Table I.

Apparatus

The ESCA apparatus used for the pulp surface characterization is an ESCALAB Mk II spectrometer, fitted on a Microlab system from Vacuum Generators and equipped with a nonmonochromatized dual Mg—Al anode X-ray source. Kinetic energies were measured by a hemispherical electrostatic analyzer ($r = 150$ mm) in the constant pass energy (20 eV) mode with a resolution of 1.1 eV. The base pressure was 10^{-8} – 10^{-6} Torr. The PE fiber was introduced into a stainless-steel cup, then into the vacuum system. Before analysis, samples were cooled for 20 min at a temperature of about -80°C . This yields a minimal sample degradation. All analyses were done with a $\text{MgK}\alpha$ source at 300 W.

FTIR results were obtained with a Mattson spectrometer, Model Sirius 100. Infrared spectra were recorded in transmittance units in the range 400–4000 cm^{-1} , with 4 cm^{-1} resolution and 300 scans with triangular apodization. PE fiber was dispersed in a tablet of KBr prepared by grinding the sample (3 mg of anhydrous fiber) with KBr (197 mg) and compressing the whole into a transparent tablet. Compression time and pressure were 15 min and 15,000 psi, respectively, and this was done using an evacuated die.

Thermal analysis was done on a Mettler TA 4000 Thermal Analysis System interfaced with a com-

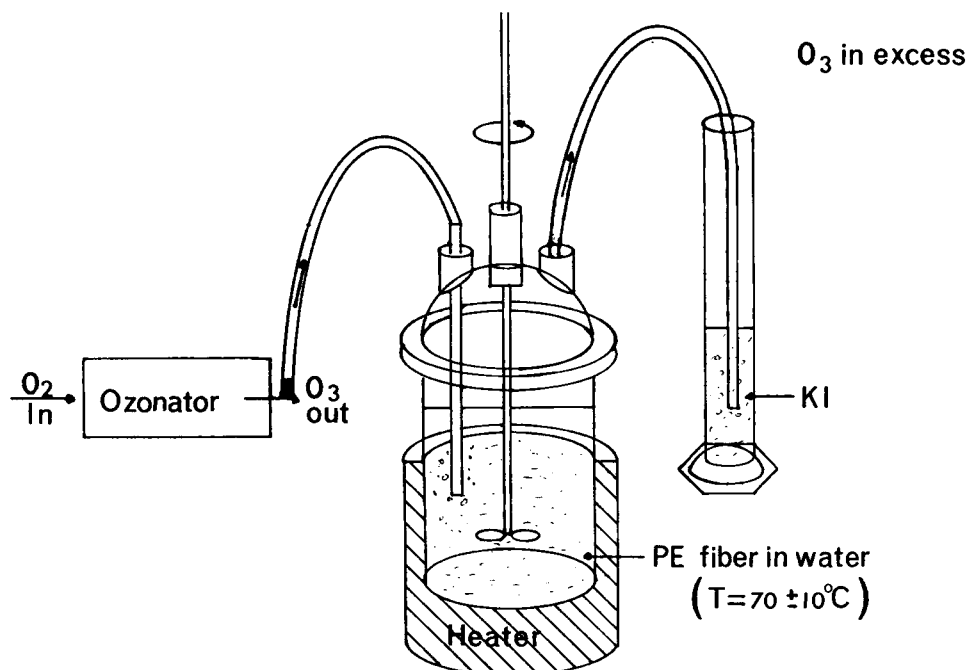


Figure 1 Schematic representation of PE pulp fiber ozonation.

puter using Mettler GraphWare TA72. Four milligrams of PE fiber were enclosed in Mettler ME-27331, 40 μL capsules. The temperature range as scanned was 40–300°C.

RESULTS AND DISCUSSION

ESCA Results and Data Treatment

The binding energy, E_b (eV), of an electron on its original shell calculated through an X-ray photoelectron technique is given by the following equation:

$$E_b = E_x - (E_k + E_c + \Phi) \quad (1)$$

Table I Description of Synthetic Pulp Fiber Used in This Study for Recording the ESCA and FTIR Spectra

Samples	Description
A	PE fiber (PE/PVA/PVAc) as received and washed by lukewarm water
B	Modified by ozone treatment during 1 h
C	Modified by ozone treatment during 2 h
D	Modified by ozone treatment during 3 h
E	Modified by ozone treatment during 4 h
F	Modified by ozone treatment during 5 h

where E_x is equal to the incident photons energy (1253.6 eV in this work for the Mg source); E_k , the kinetic energy of the electrons leaving the sample surface; E_c , the energy lost in counteracting the potential associated with the steady charging of the surface; and Φ , the work function of the spectrometer.

O/C Atomic Ratio and C_{1s} Spectra

ESCA spectra of elements detected on fiber surfaces are illustrated in Figure 2. A comparison between high-resolution C_{1s} spectra obtained at the beginning and the end of each analysis shows no sample degradation during spectra recording.

Doris and Gray¹² reported that the atomic ratio O/C of oxygen and carbon at the surface level analyzed by ESCA can be estimated from their respective peak intensities (areas) by the following equation:

$$\frac{\text{O}}{\text{C}} = \frac{1}{2.85} \times \frac{I_{\text{O}}}{I_{\text{C}}} \quad (2)$$

where $\frac{1}{2.85}$ is a correction term for the photoionization cross section. However, this equation does not take into account other correction terms related to the attenuation length, the angular asymmetry, etc.

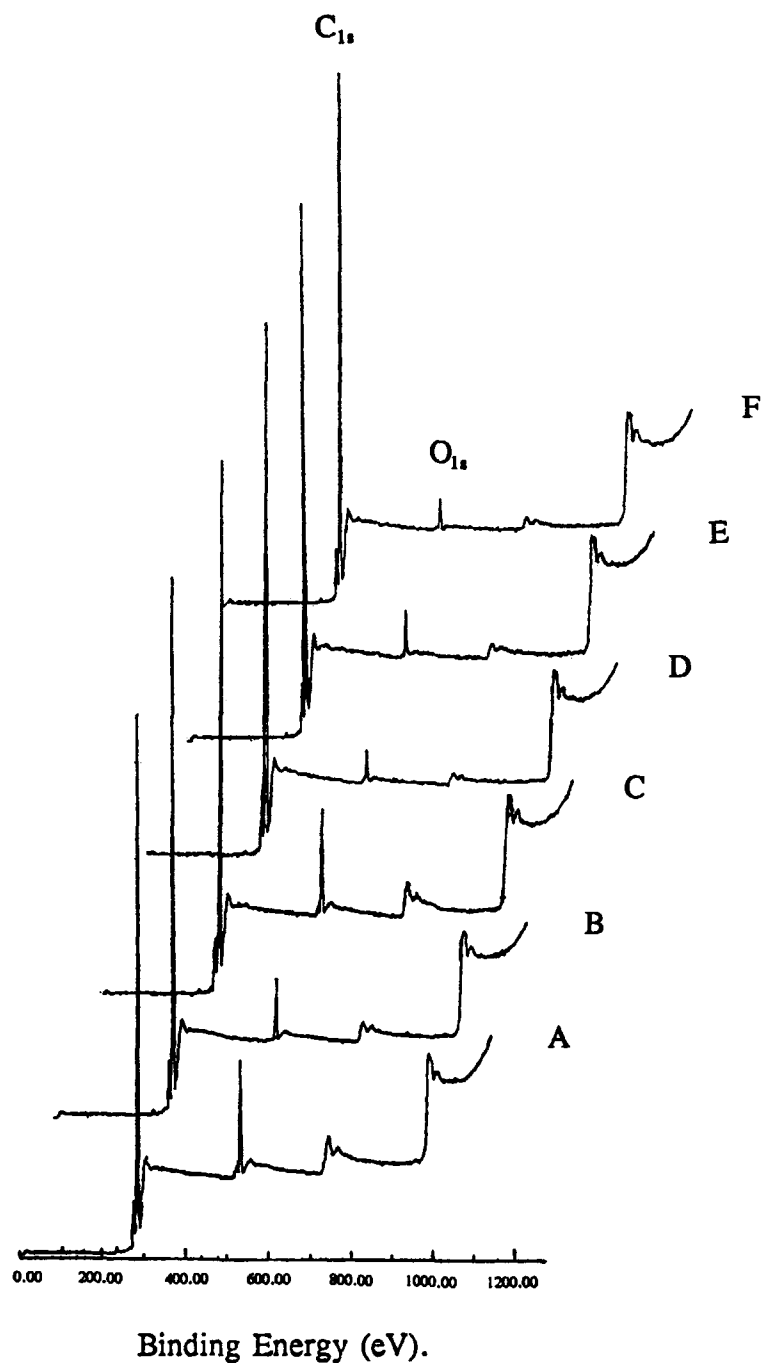


Figure 2 ESCA C_{1s} and O_{1s} spectra as intensity vs. binding energy expressed in eV of nonmodified (A) and ozonated fiber (B-F).

In this work, atomic concentrations of elements are calculated through their peak areas (intensities), taking into account²² a relative sensitivity term as mentioned in eqs. (3-5). These concentrations are qualified as apparent because the composition in the analyzed volume (around $50 \text{ mm}^2 \times 5 \text{ nm}$) is considered homogeneous.

Apparent surface concentrations of elements detected by ESCA are presented in Table II. These concentrations were calculated automatically using a special program developed in the X-ray photoelectron (GRAPS) laboratory. After entry of recording conditions of the high-resolution spectra, the program normalized peak intensities (areas).

Table II Apparent Concentrations of Elements Detected by ESCA on Surfaces of Untreated (A) and Ozone-treated Fiber (B-F)

Samples	Detected Elements (% Atomic)			
	C	O	Si ^a	Na ^a
A	90.6	9.0	0.4	—
B	94.4	5.4	—	0.2
C	92.4	7.6	—	—
D	96.6	2.8	0.6	—
E	95.7	3.9	0.4	—
F	97.0	2.9	0.1	—

^a Elements detected with very low concentrations.

This normalization is necessary if the high-resolution spectra (C_{1s} and O_{1s}) are recorded with different acquisition conditions:

- Δe : step size (= 0.1 eV, in this work)
- Δt : time per channel (= 50 ms per channel, in this work)
- n : scan number (23–50 scans, in this work)

Automatic normalization of peak intensities (areas) is made according to the following expression:

$$I_N = I_M \times \frac{\Delta e}{n \times \Delta t} \quad (3)$$

where I_N and I_M are normalized and measured intensities, respectively. Based on the following equation,²²

$$I_{XPS} = k \cdot N \cdot \sigma \cdot L \cdot \lambda \cdot T \cdot D \cdot J = k \cdot x \cdot S \quad (4)$$

where k is a proportionality term; N , the atomic density of element, related to concentration X ; σ , the photoionization cross section; L , a correction due to angular asymmetry; λ , the attenuation length; T , the analyzer transmission; D , the detector efficiency; J , the incident flux of X photons on the analyzed surface; x , the molar fraction; and S , a relative sensitivity term (= $\sigma \cdot L \cdot \lambda \cdot T \cdot J$), the program calculates the relative elementary concentrations using the following expression:

$$X_a = \frac{I_a / S_a}{\sum I_i / S_i} \quad (5)$$

Since $[O] = (I_O/S_O) / \sum (I_i/S_i)$ and $[C] = (I_C/S_C) / \sum (I_i/S_i)$, then the O/C atomic ratio is given by the following equation:

$$\frac{O}{C} = \frac{S_C}{S_O} \times \frac{I_O}{I_C} \quad (6)$$

Figure 3 shows the variation of the atomic ratio O/C calculated through apparent concentrations [eq. (5)] and through a theoretical approach, discussed later, as a function of the ozonation time. The O/C atomic ratio was higher before oxidation. Oxygen should then be from hydroxyl groups ($-OH$) in poly(vinyl alcohol) (PVA), and/or from carboxyl groups ($O-C=O$) in the poly(vinyl acetate) (PVAc) that seem to be still present at the surface of the PE fiber, even after the lukewarm water wash. The decrease of the O/C atomic ratio detected by ESCA, after the first ozonation hour, suggests elimination of PVA and PVAc on the fiber surface, and this may increase the PE surface accessibility. The outermost layers lose their oxygen with the wetting agent accessible at the surface. The oxidation of the PE surface took place at the same time, and this may account for the re-increase of the O/C atomic ratio at the second ozonation hour. The decrease of the O/C atomic ratio after 2 h of ozonation suggests the loss of oxygen-containing functionalities from the PE surface, probably due to low molecular weight oxidized molecules, soluble in aqueous solution during fiber ozonation.

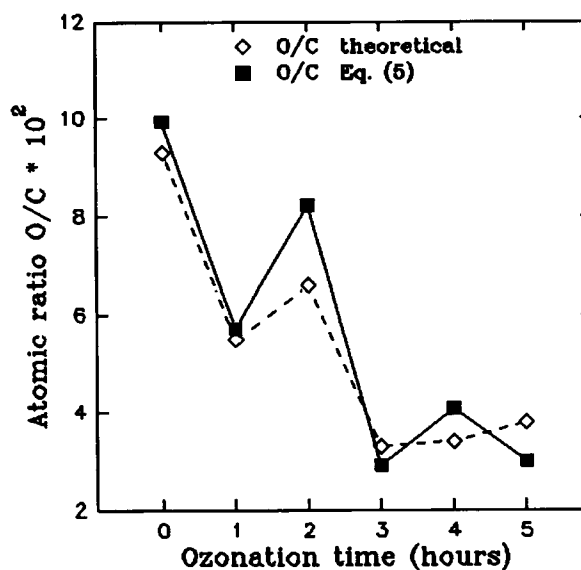


Figure 3 O/C atomic ratio at the surface of PE fiber, calculated by apparent concentrations [eq. (5)] and by a theoretical approach, as a function of the ozonation time.

A detailed examination of the C_{1s} spectra showed that these signals are composed of more than one peak. Each peak is attributed to a different chemical group. We performed spectra synthesis (Fig. 4), consisting of the addition of analytical peaks (a product of Gaussian and Lorentzian functions) in order to reproduce as near as possible the experimental spectra.³³ The adjustable parameters are

- the energy position (E_b),
- the full-width at half-maximum (ΔE_b),
- the Gauss-Lorentz ratio (G/L), and
- the peak amplitude (height).

Iwata et al.,¹⁰ citing Clark and Stephenson,¹⁸ attributed the binding energies (E_b) of 286.4, 287.8, and 289.3 eV to the carbon in the C—O groups, C=O or O—C—O groups, and O—C=O groups, respectively. Dilks³⁴ gave the carbon binding energies in the following groups:

C2: —C—O—: 286.6 ± 0.2 eV,

C3: —C=O: 287.8 ± 0.2 eV,

—O—C=O: 289.0 ± 0.2 eV,

C4: $\begin{array}{c} \text{O} \\ | \\ \text{O}=\text{C} \\ | \\ \text{O} \end{array}$: 290.6 ± 0.2 eV.

Doris and Gray¹² evaluated the chemical shifts of the C_{1s} peak components relative to the value of 285.0 eV for the C1 (C—C) component of the C_{1s} peak. Choosing this value is equivalent to referencing the binding energy scale to the value of 533.2 eV for the O2 component of the O_{1s} peak. In this work, we chose 285.0 eV as the binding energy for the C1 component of the C_{1s} peak components, and we correct the binding energies of C2 and C3 (Table III), as well of O0, O1, and O3 (Table IV) relative to it.

Tables III and IV present the results of the C_{1s} and O_{1s} peak synthesis, respectively; all energies (E_b , ΔE_b) are in eV, and % represents the percentage of each component with regard to the considered element. In these tables, the E_b were corrected with the hypothesis that the C1 component, representing C—C and C—H bindings, corresponds to a binding energy of 285.0 eV.¹²

Graphical results of the peak synthesis are presented in Figures 4 and 5. Three components are observed for the C_{1s} spectra (Fig. 4): The C1 com-

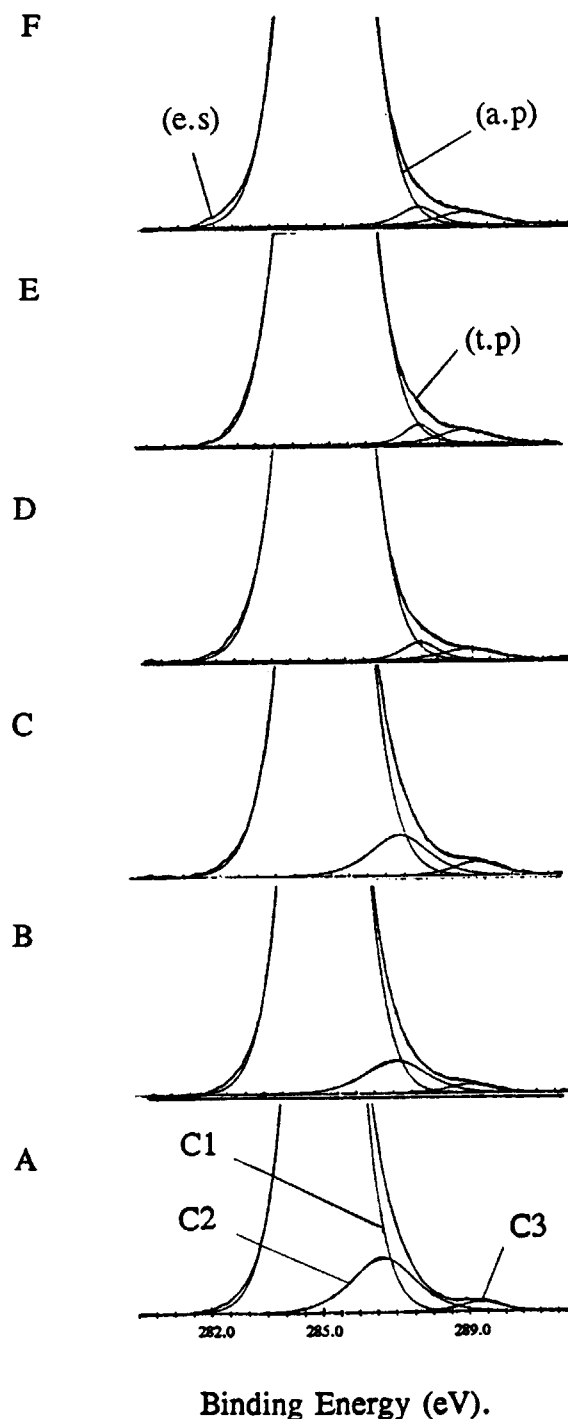


Figure 4 ESCA C_{1s} spectra as intensity vs. binding energy expressed in eV: experimental spectrum (e.s); total peak synthesis (t.p); analytical peaks (a.p) of nonmodified (A) and ozonated fiber (B–F).

ponent is attributed to aliphatic carbon $(CH_2)_n$, whereas C2 and C3 are attributed to carbon-oxygen bonds. It is evident from Figure 4 that, even after

Table III Corrected Binding Energies E_b (eV), fwhm ΔE_b (eV), Gauss/Lorentz (G/L) Ratio, and Fractional Area for Deconvolution Components from ESCA C_{1s} Peaks of Untreated (A) and Ozone-treated Fiber (B–F)

Samples	Carbon C_{1s} Peaks											
	C1				C2*				C3 ^b			
	E_b	ΔE_b	G/L	%	E_b	ΔE_b	G/L	%	E_b	ΔE_b	G/L	%
A	285.0	1.60	.58	91.6	286.6	2.10	.58	7.5	289.3	1.3	.58	0.9
B	285.0	1.63	.54	95.3	287.0	1.95	.54	3.9	289.0	1.5	.54	0.8
C	285.0	1.68	.63	94.6	287.1	1.83	.63	4.2	289.2	1.5	.63	1.2
D	285.0	1.77	.54	97.8	287.6	1.12	.54	1.1	289.0	1.8	.54	1.1
E	285.0	1.76	.56	97.8	287.5	0.95	.56	1.0	288.8	1.6	.56	1.2
F	285.0	1.74	.56	97.5	287.6	1.18	.56	1.2	288.9	1.8	.56	1.3

* Based on the E_b , C2 = C3^a for samples D–F.

several hours of ozonation, aliphatic carbon, as C1, is still dominant on the surface.

Following Dilks,³⁴ C3 is attributed to the binding energies of 287.8 ± 0.2 and 289.0 ± 0.2 eV. We define C3^a and C3^b, and we associate them to the two last binding energies, respectively. From Table III, C3 could be associated to C3^b (O—C=O) and this is based on the binding energy being relatively the same. C3^b (carbon in carboxyl groups) concentration increases from 0.9% on the nonozonated fiber (sample A) to 1.3% on the 5 h ozonated fiber. Carboxyl groups on sample A are proof of the presence of PVAc on the nonozonated fiber surface. This is due to carboxyl groups introduced at the end of PE chains. Table III also shows that the binding energies for C2 are relatively higher, compared with Dilks's³⁴ value, especially at high ozonation times (D, E, and F). There is (Table III) an increase in

C2 binding energies as ozonation time increases. A shift of 0.5 eV in C2 binding energy between sample C (ozonation time = 2 h) and D (3 h) is observed. This shift is equal to 1.0 eV if the comparison is done between sample A (nonozonated fiber) and sample D. The C2 binding energies of samples D, E, and F are relatively the same as the binding energy attributed by Dilks³⁴ to C3 (here, C3^a: C=O). Samples D, E, and F seem to be different from other samples (A, B, and C). This difference is remarkable on for the C2 component, which increases in binding energies and decreases in ΔE_b . Thus, we see (Table III, C2) two series of binding energies changing from about 287.0 to about 287.6 eV between 2 and 3 h ozonation time. There is the same discontinuity in the ΔE_b from about 2.0 to 1.0 eV. There is an increase in the oxidation state of the carbon atoms, in a rather discontinuous manner at these times. These changes

Table IV Corrected Binding Energies E_b (eV), fwhm ΔE_b (eV), Gauss/Lorentz (G/L) Ratio, and Fractional Area for Deconvolution Components from ESCA O_{1s} Peaks of Untreated (A) and Ozone-treated Fiber (B–F)

Samples	Oxygen O_{1s} Peaks											
	O0				O1				O2			
	E_b	ΔE_b	G/L	%	E_b	ΔE_b	G/L	%	E_b	ΔE_b	G/L	%
A	—	—	—	—	532.4	1.8	.75	44.0	533.2	1.8	.77	56.0
B	—	—	—	—	532.3	1.9	.83	51.5	533.2	1.9	.80	48.5
C	—	—	—	—	532.3	1.9	.80	49.4	533.2	1.9	.80	50.6
D	—	—	—	—	532.4	2.0	.80	59.5	533.4	2.0	.85	40.5
E	—	—	—	—	532.4	2.1	.80	66.6	533.3	2.1	.82	33.4
F	529.4	2.2	.80	8.1	532.4	2.1	.80	49.5	533.4	2.1	.80	42.4

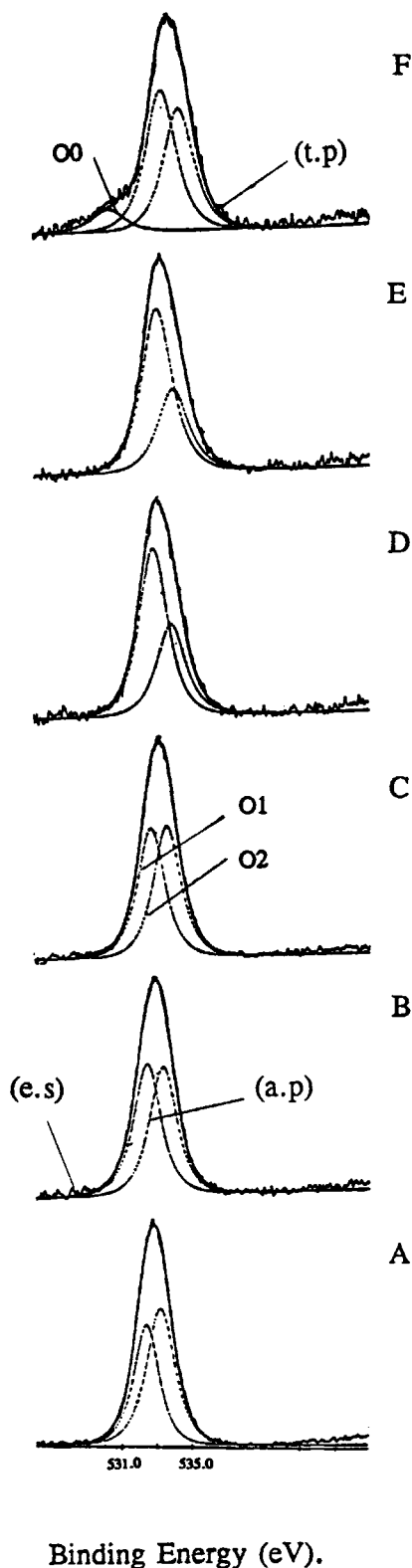


Figure 5 ESCA O_{1s} spectra as intensity vs. binding energy expressed in eV: experimental spectrum (e.s); total peak synthesis (t.p); deconvoluted peaks (d.p) of non-modified (A) and ozonated fiber (B–F).

are also in evidence in FTIR measurements, as shown later.

As a test of self-consistency, we define R , as an atomic ratio, and Q , as a sum of atomic ratios, based on stoichiometric relations between c_2 , c_3 , and O/C as

$$R = O/C, \quad \text{and}$$

$$Q = 1c_2(\%) + 1c_3^a(\%) + 2c_3^b(\%) \quad (7)$$

where $c_2(\%) = [C_2]/[C]$; $c_3(\%) = [C_3]/[C]$; $c_3^a(\%) = [C_3^a]/[C]$; and $c_3^b(\%) = [C_3^b]/[C]$. In eq. (7), numbers in front of concentrations are the number of oxygen atoms per each carbon atom. R should be equal to Q for all samples. For samples A, B, and C, $Q = 1c_2 + 2c_3^b$ ($c_3^a = 0$), whereas $Q = 1c_3^a + 2c_3^b$ ($c_2 = 0$) for the remaining samples. Table V shows that R is not quite equal to Q . This could be explained in three ways:

- Not enough precision in the deconvolution of the C_{1s} spectra and the evaluation of C_2 and C_3 peak areas, which are very small compared with those of the C_1 component.
- Presence of oxygenated species, adsorbed at the PE fiber surface, whose O_{1s} binding energy is not so different from the energy of the oxygen bonded with carbon.
- Presence of anhydride moieties ($O=C-O-C=O$), in which two atoms of carbon (C_3^b) correspond to only three atoms of oxygen, rather than to four.

O_{1s} Spectra

The envelope of the oxygen O_{1s} spectra (Fig. 5) reveals two main components: O1 at 532.3 and 532.4 eV and O2 at 533.3 ± 0.1 eV. A binding energy of 533.2 eV attributed to the O2 component of the O_{1s}

Table V Apparent Concentration Ratio O/C (R) and Theoretical O/C Values (Q) Estimated from C_2 and C_3 Fractional Area of Untreated (A) and Ozonated Fiber (B–F)

Samples	R (%)	Q (%)
A	9.9	9.3
B	5.7	5.5
C	8.2	6.6
D	2.9	3.3
E	4.1	3.4
F	3.0	3.8

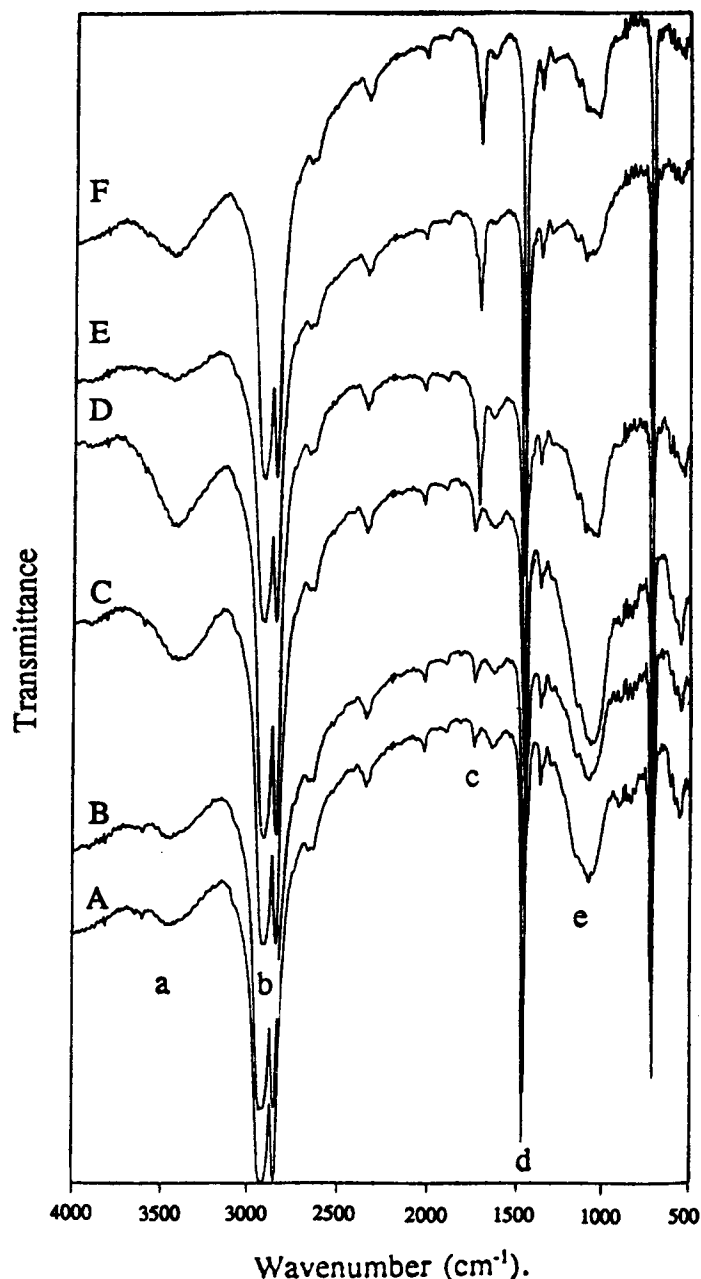


Figure 6 FTIR spectra of (A) nonmodified and (B-F) ozonated fiber: (a) O—H valence vibration; (b) C—H valence vibration; (c) C=O valence vibration; (d) CH₂ deformation vibration; (e) C—O valence vibration.

peak is frequently reported in the literature.¹²⁻²⁰ The binding energies of the O2 component measured in this work and corrected, based on the binding energy of 285.0 eV attributed to C1, correlate very well with the literature.¹²⁻²⁰ O2 components arise from the hydroxyl (OH) oxygen, whereas O1 components arise from the other oxygens such as (O=C and/or —O—). It should be pointed out that, for non-ozonated fiber, the surface is richer in hydroxyl

groups (Table IV, A: O2/O = 56% and O1/O = 44%, where O corresponds to the total oxygen concentration). This reveals the presence of PVA and PVAc at the surface.

The decrease of O2/O vs. the increase of O1/O after the first hour of ozonation can be a sign of the elimination of PVA, and, therefore, of hydroxyl groups, as discussed above. Table IV shows an important increase in the O1/O ratio for sample D (3

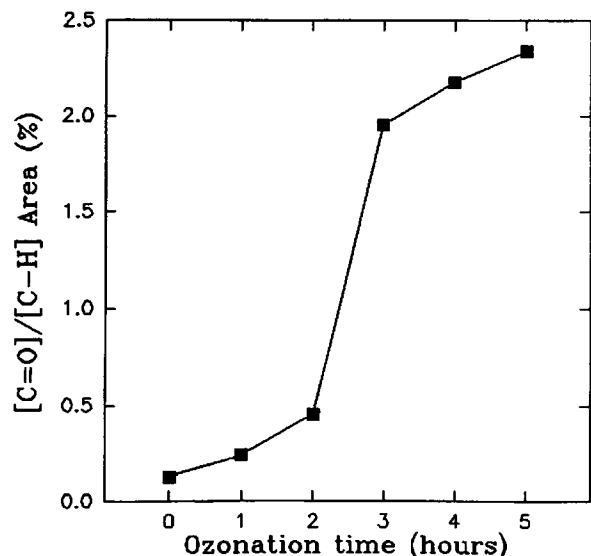


Figure 7 Carbonyl band ($1740\text{--}1700\text{ cm}^{-1}$, valence vibration), relative to hydrocarbon band ($2930\text{--}2852\text{ cm}^{-1}$, valence vibration) area, as a function of the ozonation time.

h of ozonation) and especially for sample D (4 h). This should be accompanied by a significant variation in surface energy.

An important result is revealed also by Table IV. It is the onset of a new component for the O_{1s} peak (Fig. 5; F), with a lower binding energy, at 529.4 eV. We attribute this binding energy to OO components probably arising from oxygen bonded with a double bond (carbonyl) involved in a hydrogen bond with a neighboring hydroxyl group ($-\text{O}-\text{H}\cdots\text{O}=\text{C}$). This results in a lower binding energy. The existence of intra- and intermolecular hydrogen bonds is a highly probable phenomena after a long time of oxidation (5 h) by ozone. A similar binding energy ($\approx 530.2\text{ eV}$) has been associated to the OO component by Ahmed et al.³⁵ in a study of the solid residues of supercritical extraction of *Populus tremuloides* in methanol. They believe that it could be attributed to the oxygen in strongly adsorbed water.

FTIR Analysis

To determine the level of modification caused by ozone treatment on PE fiber, FTIR spectroscopy measurements were performed as a function of reaction time. FTIR spectra of all samples are illustrated in Figure 6. This figure shows that the vibrational bands that are significantly perturbed as a function of ozone treatment time are the carbonyl band vibrations at about $1740\text{--}1700\text{ cm}^{-1}$. It should

be pointed out that no spectrum is free from carbonyl band vibrations, but the intensity of this band increased relatively from one sample to another as a function of reaction time. Here, in the FTIR analysis, we mean by the word intensity the height of the peak and not the area as in the ESCA analysis. The carbonyl band area is measured relatively to the hydrocarbon (C—H) band area, and the result is shown in Figure 7, as a function of the ozonation time. In this figure, a large increase in the $[\text{C}=\text{O}]/[\text{C}-\text{H}]$ area at the third hour of reaction can be observed. As discussed above (ESCA results) with O/C atomic ratio, two series of fiber stand out through this discontinuity in the $[\text{C}=\text{O}]/[\text{C}-\text{H}]$ area ratio. However, Figure 3 showed an outstanding decrease in the O/C atomic ratio at this time of

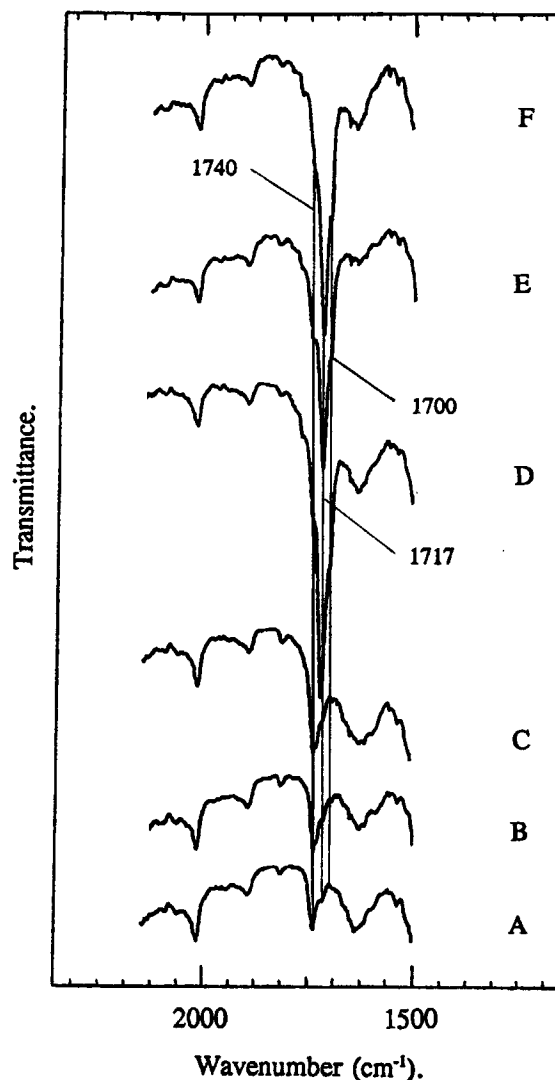


Figure 8 FTIR spectra focused on carbonyl band of (A) unmodified and (B–F) ozonated fiber.

phology of the fiber, caused by the large oxidation reaching the bulk when exceeding 2 h of ozonation.

CONCLUSIONS

ESCA and FTIR spectra of PE fiber reveal well the effect of the ozonation on the fiber chemical history at the surface and the bulk. Synthetic pulp fiber, used as the ozonation substrate in this study, was not pure PE. The presence of a wetting agent, i.e., PVA/PVAc, at the outermost layers level was detected by FTIR and confirmed by the ESCA technique.

The C_{1s} and O_{1s} spectra are useful tools for analyzing the surface oxidation and complement each other. The OO component of the O_{1s} spectra, for sample F, could not be detected by only C_{1s} synthesis (C2 and C3). The atomic ratio O/C decreasing after 1 h of ozonation indicates the elimination of the PVA/PVAc, which is more accessible at the surface. The increase of O/C after the second ozonation hour indicates the oxidation of the PE surface.

The third hour was a critical time in the oxidation process. It was marked by a significant increase in the carbonyl band vibrations detected by FTIR. On the other hand, ESCA detects only a low atomic ratio O/C.

The appearance of the band attributed to moieties of conjugated aldehyde at 1700 cm^{-1} and the drastic

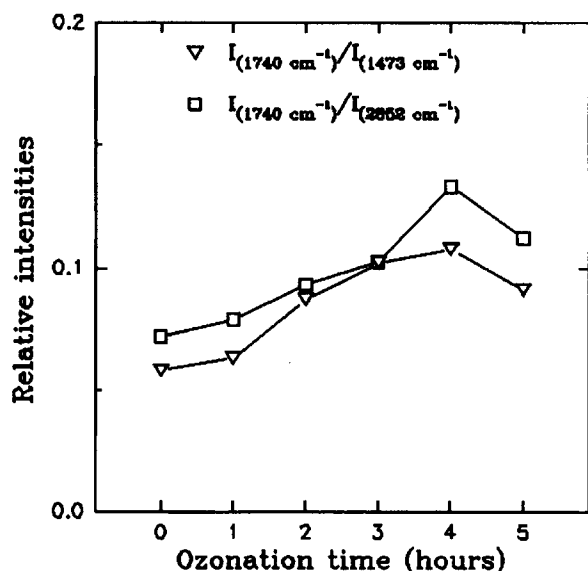


Figure 11 Intensity of the nonconjugated aldehyde [HRC=O] band (1740 cm^{-1}), relative to the intensities of [C—H] (2852 cm^{-1} , valence vibration) and of [—CH₂—] (1473 cm^{-1} , deformation vibrations) bands, as a function of the ozonation time.

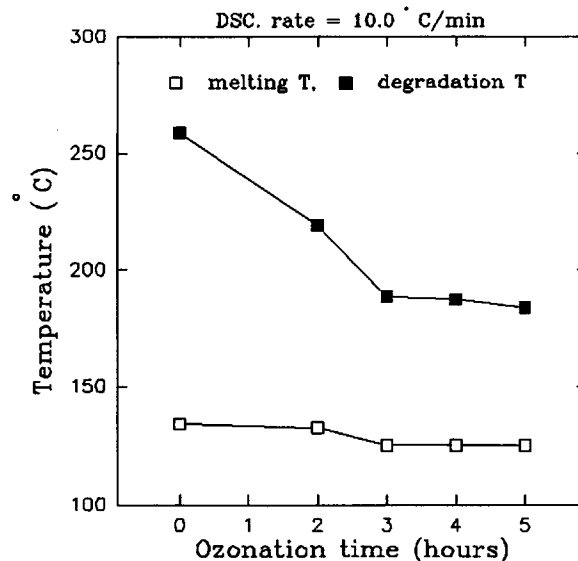


Figure 12 Melting and degradation temperatures of nonmodified and ozonated fiber, as a function of the ozone treatment time.

increase in nonconjugated ketone (R'RC=O) intensity at 1717 cm^{-1} , at the third ozonation hour, are proof of chain scission and ablation and the oxidation of the chains. Oxygen-containing functionalities were lost at the third hour of ozonation, from the outermost layers level, whereas the bulk was largely oxidized. Thermal analysis indicates that exceeding 2 h of ozone treatment affects the structure and the morphology of the macromolecules of the PE fiber.

Further studies are underway to determine the variation of surface energies vs. the variation of the chemical composition caused by the ozone treatment, as well as composite paper characteristics.

The authors thank DuPont for the generous gift of the synthetic pulp fiber, as well as A. E. Hughes and B. A. Sexton³³ for their free program given to the Groupe de Recherche sur les Applications de la Physico-chimie des Surfaces, used for ESCA data analysis, and the Natural Sciences and Engineering Research Council of Canada and le fonds pour la formation de chercheurs et l'aide à la recherche of Quebec and the Tunisian Government for financial support.

REFERENCES

1. S. Dasgupta, *J. Appl. Polym. Sci.*, **41**, 233 (1990).
2. D. L. Forbess, W. A. Kindler, and R. A. Marti, U.S. Pat. 3,848,027 (1974).

3. T. Rave, in *Kirk-Othmer Encyclopedia of Chemical Technology*, M. Grayson, Ed., Wiley, New York, 1978, Vol. 19, p. 425.
4. T. Fujita, H. Ishida, T. Kamaishi, and S. Otsu, Ger. Pat. 2,649,139 (1977).
5. P. Pirro, Belg. Pat. 824,531 (1974).
6. G. Voituron and J. P. Pleska, Ger. Pat. 2,649,139 (1975).
7. E. Agouri, R. Laputte, and J. Rideau, U.S. Pat. 4,080,405 (1978).
8. D. K. Owens, *J. Appl. Polym. Sci.*, **19**, 3315 (1975).
9. J. F. Carley and P. T. Kitze, *Polym. Eng. Sci.*, **20**, 330 (1980).
10. H. Iwata, A. Kishida, M. Suzuki, Y. Hata, and Y. Ikada, *J. Polym. Sci. Polym. Chem. Ed.*, **26**, 3309 (1988).
11. Y. Uyama and Y. Ikada, *J. Appl. Polym. Sci.*, **36**, 1087 (1988).
12. G. M. Doris and D. G. Gray, *Cell. Chem. Technol.*, **12**, 72 (1978).
13. A. Ahmed, A. Adnot, J. L. Grandmaison, S. C. Kaliaguine, and J. Doucet, *Cell. Chem. Technol.*, **21**, 483 (1987).
14. D. N. S. Hon, *J. Appl. Polym. Sci.*, **29**, 2777 (1984).
15. A. O. Barry, B. Riedl, A. Adnot, and S. C. Kaliaguine, *J. Elect. Spect. Rel. Phenom.*, **57**, 47 (1991).
16. D. P. Kamdem, B. Riedl, A. Adnot, and S. C. Kaliaguine, *J. Appl. Polym. Sci.*, **43**, 1901 (1991).
17. G. Qu Xiang Yang, PhD Thesis, Kansas State University, Manhattan, 1987.
18. D. T. Clark and P. T. Stephenson, *Polymer*, **23**, 1034 (1982).
19. D. T. Clark and I. Ritchie, *J. Polym. Sci. Polym. Chem. Ed.*, **13**, 857 (1975).
20. D. T. Clark, *Adv. Polym. Sci.*, **24**, 125 (1977).
21. A. P. Pijpers and W. A. B. Donners, *J. Polym. Sci. Polym. Chem. Ed.*, **23**(2), 453 (1985).
22. D. Briggs, in *Practical Surface Analysis by Auger and X-ray Photoelectron Spectroscopy*, D. Briggs and M. P. Seah, Eds., Wiley, New York, 1983.
23. D. M. Soignet, R. J. Berni, and R. R. Benerito, *J. Appl. Polym. Sci.*, **20**, 2483 (1976).
24. Y. Uyama and Y. Ikada, *J. Appl. Polym. Sci.*, **36**, 1087 (1988).
25. J. F. Elman, L. J. Gerenser, K. E. Goppert-Berarducci, and J. M. Pochan, *Macromolecules*, **23**, 3922 (1990).
26. E. Uchida, Y. Uyama, H. Iwata, and Y. Ikada, *J. Polym. Sci. Polym. Chem. Ed.*, **28**, 2837 (1990).
27. F. G. Hurtubise, *Tappi J.*, **45**, 460 (1962).
28. C. Y. Liang and R. H. Marchessault, *J. Polym. Sci.*, **39**, 269 (1959).
29. H. I. Bolker and N. G. Sommerville, *Pulp Paper (Can)* T187 (1963).
30. A. J. Michell, *Appita*, **39**, 223 (1986).
31. S. C. Lin, B. J. Bulkin, and E. M. Pearce, *J. Polym. Sci. Polym. Chem. Ed.*, **17**, 3121 (1979).
32. D. J. Jenkin, *Appl. Polym. Symp.*, **28**, 1309 (1976).
33. A. E. Hughes and B. A. Sexton, *J. Electr. Spectr. Relat. Phenom.*, **46**, 31-42 (1988).
34. A. Dilks, in *Developments in Polymer Characterisation-2*, J. V. Dawkins, Ed., Applied Science, London, England, 1980, p. 145.
35. A. Ahmed, A. Adnot, and S. Kaliaguine, *J. Appl. Polym. Sci.*, **34**, 359-375 (1987).

Received June 2, 1992

Accepted September 26, 1992